Theor Chem Acc (2010) 127:605–612
DOI 10.1007/s00214-010-0756-0

REGULAR ARTICLE

Theoretical study of challenging properties of intramolecularly π-stacked oligo(dibenzofulvene) organic molecular semiconductors

J. C. Sancho-García

Received: 22 February 2010 / Accepted: 6 April 2010 / Published online: 22 April 2010

Abstract It has been recently argued that poly(dibenzofulvene) displays different properties for inter- and intrachain charge transport processes in the hopping regime. The charge carrier path for intramolecular transport consists in a set of π-stacked fluorene rings attached as pendant groups to the main chain, which defines a set of increasingly longer oligomers of helical shape according to the number of fluorene rings. The all-pervasive non-covalent interactions, influencing the mutual orientation of the π-stacked fluorene rings, is accounted for by dispersion-corrected methods, which had to be previously assessed against some experimental values. The present theoretical study aims to rationalize the competition between the two processes (inter- vs. intrachain) through the accurate calculation of the molecular parameters governing charge transport along the intrachain path. Finally, we perform a computationally guided molecular engineering of a set of molecules, not yet synthesized, with extended face-to-face π-stacking, which is achieved by fusing benzene rings to terminal sides of the fluorene moieties. This allows us to anticipate the performance of this new set of related materials.

Keywords Density-functional theory · Non-covalent interactions · π-stacked conjugated molecules · Intramolecular charge transport process · Intrachain mobilities

J. C. Sancho-García (✉)
Departamento de Química Física,
University of Alicante,
03080 Alicante, Spain
e-mail: jc.sancho@ua.es

1 Introduction

The field of molecular and plastic electronics is largely based on the intrinsic conducting properties of functional organic molecules and conjugated polymers, which are able to act as active layers of optoelectronic devices after sandwiching between two electrodes. Organic semiconductors have even surpassed amorphous silicon in performance [1, 2] and many technologically relevant applications are envisioned or are commercially available now. The theoretical framework used to describe the charge transport mechanism in these materials shares the formalism with the field of electron-transfer reactions, which is known to play a central role in many scientific fields [3]. Much interest is currently devoted to exploit the π-stacking interactions found between neighbouring molecules as a driving force for increasing charge carrier mobilities, which is known to play a leading role in the efficiency of these devices [4, 5]. In fact, some of the highest performances recently achieved in organic field-effect transistors are indeed due to ultra close π-stacking and favourable molecular orientation found in the films [6–8]. It is hoped that the highest carrier mobilities reported to date might be further increased by fine-tuning the solid-state packing or after appropriate chemical functionalization; note that non-covalent intermolecular interactions between the planar or rigid-rod π-conjugated motifs ultimately dominate the preferred solid-state packing of these materials.

On the other hand, a new class of covalently bridged π-stacked fluorene systems called oligo(dibenzofulvenes), oligo(DBF), see Fig. 1, was recently synthesized [9, 10], and their properties widely characterized [11, 12], as promising and versatile charge transport materials [13–15]. These model compounds are intended to serve as

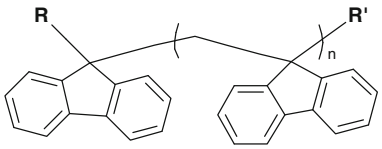

n	R	R'	
1	H	H	DBF dimer (A)
1	CH_3	CH_3	DBF dimer (A')
2	CH_3	CH_3	DBF trimer (B)
2	H	C_5H_{11}	DBF trimer (B')
3	CH_2Ph	C_5H_{11}	DBF tetramer (C)
4	CH_2Ph	CH_2Ph	DBF pentamer (D)
5	C_2H_5	C_2H_5	DBF hexamer (E)

Fig. 1 Chemical structures and nomenclature of the investigated compounds. The hydrogen atoms have been omitted for clarity

prototypes for studying and further engineering intramolecular interactions, which might largely drive the experimental hole drift mobilities measured [16, 17]. In the film sample, both intra- and intermolecular processes are expected to take place. In fact, a fast exchange of a single electron among several fluorene moieties belonging to the same chain, probably assisted by tunnelling, has been recently observed [18]. We have thus systematically investigated here, at a full quantum-chemical level, how the orientation of the cofacial fluorene units evolves with the nature and size of the system and if this feature introduces undesired disorder effects for long oligomers approaching the polymer limit.

Note that a detailed and accurate investigation of these materials still represents a challenge for any theoretical method [19]. Organic electronic materials are often used as a class of p-type systems; note that charge transport is expected in these materials to be more efficient for holes than for electrons [20]. Notwithstanding the above-mentioned features, we need to reliably estimate the molecular parameters governing the rate of charge hopping between two adjacent fluorene rings belonging to the same chain, which is based on [21]: (i) the electronic intramolecular coupling between the frontier electronic levels, also known as transfer integral, and (ii) the energy change as a result of the geometry distortions experienced during the charge hopping. Note that the molecular geometries and energies are expected to be poorly described by those methods unable to accurately account for non-covalent interactions; these interactions, on the other hand, are expected to highly influence the final shape of the chains. Thus, we must first to select the method to be applied, based on a detailed assessment of the strengths and drawbacks of available theoretical methods, for the understanding of supramolecular structures and energetics, which is done next.

2 Computational details

We present here a summary of the DFT-based exchange-correlation functionals employed along this work. The Generalized Gradient Approximation (GGA) is treated as a baseline for further developments. Among all the available expressions we select the ubiquitous B88 [22] and LYP [23] for exchange and correlation functionals, $E_x[\rho]$ and $E_c[\rho]$, respectively. The expression adopted to systematically introduce additional components within the functional is as general as:

$$E_{xc}^{\text{double-hybrid}}[\rho] = w_{HF}E_x^{HF} + (1 - w_{HF})E_x[\rho] \quad (1)$$

$$+w_{PT2}E_c^{PT2} + (1 - w_{PT2})E_c[\rho], \quad (2)$$

where E_x^{HF} and E_c^{PT2} are, respectively, the exact exchange HF-like energy and the correlation energy obtained at the Møller–Plesset perturbation theory up to second order [24]. Note that both terms are evaluated with the orbitals arising from the solution of the Kohn–Sham one-electron equations [25]. The E_c^{PT2} perturbative term has the form:

$$E_c^{PT2} = \frac{1}{4}\sum_{ia}\sum_{jb}\frac{[(ia|jb) - (ib|ja)]^2}{\epsilon_i + \epsilon_j - \epsilon_a - \epsilon_b}, \quad (3)$$

where *ij* and *ab* refer to occupied and virtual spin orbitals, respectively, and ε are the corresponding orbital energies. Note that these double-hybrid functionals (B2-PLYP), in the sense that both exchange and correlation are combined with expressions taken from ab initio theories, belong to a higher rung in the hierarchy of DFT-based methods than pure or hybrid functionals do [26]; the latter being found if $w_{PT2} = 0$ but $w_{HF} \neq 0$. These orbital-dependent functionals are called to play a major role in next decades due to their flexibility and proved accuracy [27–30]. Table 1 presents the detailed composition of the exchange-correlation functionals used in this work. Note that the values for w_{HF} and w_{PT2} are always obtained by fitting to a well-defined training set. A newly reparameterized $B_\lambda LYP$

Table 1 Detailed composition of the exchange-correlation functionals used in this work

Type	Functional	w_{HF}^a	w_{PT2}^b	E_x [ρ]	E_c [ρ]
Semilocal GGA	B	0	0	B	–
	BLYP	0	0	B	LYP
Hybrid GGA	B3LYP	0.20	0	B	LYP,VWN
	$B_\lambda LYP$	0.2533	0	B	LYP
	BHHLYP	0.50	0	B	LYP
Double-hybrid GGA	B2-PLYP	0.53	0.27	B	LYP

[a] Weight of the HF-like exchange. Formal scaling by N^4, without further approximations, where N is related to the size of the molecule

[b] Weight of the perturbative term. Formal scaling by N^5, without further approximations, where N is related to the size of the molecule

functional, which was recently devised specifically for calculations of charge transport properties of organic molecular semiconductors [31], will be also used here to further assess its reliability. Note that B3LYP-based [32] results are also included for completeness since this functional is routinely applied nowadays. We remind that the formal scaling of these methods (N^4/N^5, where N is related to the size of the molecule) is several order of magnitude lower than ab initio methods, as CCSD(T) is, which are known to give reliable results for intermolecular π–π interactions [33] although, however, at a computational cost which precludes their application to the longest oligomers tackled here.

Regarding the technical details, all the calculations are performed with the ORCA quantum-chemical package [34] and assume that the molecules are in the gas phase. Analytical gradients are available for all the methods [35]. Density fitting techniques were applied to speed up the B2-PLYP calculations [36]; however, this approximation is not expected to introduce any meaningful error in the calculation of energy differences or geometries [37]. Concerning the choice of a basis set, we first remark that the charge transport magnitudes calculated here hardly depend on large basis sets [38, 39]. Thus, the 6-31G* basis set was fixed as a decent compromise between accuracy and computational cost. The grid for numerical integration of the exchange-correlation functional was made denser than the default to reduce numerical errors. The application of an external electric field, as normally found in molecular-based device applications, is not expected to significantly modify the conclusions, as shown in previous studies [40].

3 Results and discussion

3.1 Benchmarking the theoretical methods

We have first used crystallographic structures for the preliminary calculations in order to avoid mixing structural and electronic effects [41]. Note that it has been previously suggested that these molecules possess similar geometries in the gas phase and in the crystalline state [20]. We remind that the goal here is to assess first the reliability of the methods to select the most convenient one according to the complicated nature of the problem. Therefore, we have chosen a set of molecules (A, A′, B; i.e., the shortest oligomers shown in Fig. 1), for which a variety of experimental results are available, to conveniently assess the computational methods to be further employed. First, the measurements of gas-phase photoelectron spectra is known to provide the vertical detachment energies [9, 20] which can be readily compared to theoretical results [42]. On the other hand, the comparison of theoretically calculated vertical excitation energies ($E_{S_1} - E_{S_0}$) in vacuum with the lowest-energy absorption peak (E_{00}) at room temperature and using THF as solvent [10], requires further manipulations [43]. First, the E_{00} values measured in solution have been increased by 0.15 eV (ΔE_{solv}) because the typical shifts, related to solvation effects, are of the order of 0.1–0.3 eV and increase with the size of the system [43]. We have then added the equilibration energy (ΔE_{eq}) in the lowest excited state extracted from absorption spectra at room temperature. Since a vibronic replica is not observed in the absorption spectra, the vertical excitation energies are expected to be close within 0.1–0.2 eV to the absorption maximum. We have thus considered an approximate averaged energy shift ($\Delta E_{solv} + \Delta E_{eq}$) of 0.3 eV, which is added to the experimental E_{00} value before comparing experimental and theoretical results.

Table 2 gathers the results for vertical ionization potentials and singlet-singlet excitation energies for the various DFT-based methods employed; the latter calculated at the corresponding time-dependent (TD-)DFT level. Note that a good description of the D_0 (radical-cation) ground state and the S_1 (first singlet) excited state is a prerequisite of any method for further application within the organic electronics field [44]. Certainly, we observe that pure functionals ($w_{HF} = w_{PT2} = 0$) lead to rather poor results for both properties. Furthermore, we see how the results for excitation energies are only marginally affected after adding the corresponding correlation functional. We have also tried a density functional with improved long-range behaviour, the LB94 expression [45], implemented through the gradient regular asymptotic correction [46], to see its effect on the GGA-based results. The orbital energies and lowest excitation energies were affected by less of 0.1 eV

Table 2 Computational estimates of vertical ionization potentials ($E_{D_0} - E_{S_0}$, in eV) and transition energies from the ground to the first excited singlet state ($E_{S_1} - E_{S_0}$, in eV)

Method	$E_{D_0} - E_{S_0}$			$E_{S_1} - E_{S_0}$		
	A	A′	B	A	A′	B
B	5.6	5.4	5.1	3.5	3.6	3.5
BLYP	6.6	6.3	6.0	3.4	3.5	3.5
B3LYP	6.9	6.7	6.4	4.3	4.3	4.2
B_λLYP	6.9	6.6	6.4	4.6	4.4	4.4
BHHLYP	7.2	6.9	–	5.1	4.8	4.8
B2-PLYP	7.3	6.9	6.8	4.9	4.6	4.7
Exp.	7.7[a]	7.5[b]	7.3[b]	–	4.3[c]	4.3[c]

All quantities are calculated with the 6-31G* basis sets

[a] Taken from [20]

[b] Taken from [9]

[c] Taken from [10] and corrected with both the solvent shift and the equilibration energy (see text for details)

and will thus not be shown; these corrections are expected to be more important in studying Rydberg states. Thus, the parameter to be controlled seems to be the addition of a moderate portion of HF-like exchange (B3LYP or B_λLYP), which significantly improves the results. However, it is also known that higher weights could lead to rapidly deteriorate the accuracy for thermochemical and other ground-state properties. Finally, the double-hybrid orbital-dependent functionals (B2-PLYP) also behaves rather accurately, as expected [47]. Note that the B2-PLYP results for excitation energies include the so-called doubles correction, which systematically improves the values by around 0.2 eV from the compensation of the large fraction of HF-like exchange. Therefore, as usual for conjugated materials [48, 49], it seems difficult to negotiate the need of different values of w_{HF} for various properties and systems.

Since the results provided by the B_λLYP functionals are of the same quality than those of the B3LYP methods, and the former is expected to give slightly better results for transport properties of conjugated systems [50], we will use in the following one representative of each class of methods, namely: BLYP (Semilocal GGA), B_λLYP (Hybrid GGA), and B2-PLYP (Double-hybrid GGA), to ascertain the transport parameters of the dibenzofulvene (DBF) oligomers. Note also that B3LYP has not been recommended for the calculation of through-space interactions between parallel arenes in peri-substituted biphenylenes [51].

3.2 Predicted structures of π-stacked DBF oligomers

The accurate description of non-covalent interactions is expected to play an increasingly leading role for the accurate description of π-stacked compounds, supramolecular assemblies, chromophore macrocycles, tubular aggregates, and guest emitters inserted in cavities or host compounds. Unfortunately, DFT has not reached yet the stage where the non-covalent interactions can be reliably and accurately predicted without further manipulations [52–54]. Note that calculations with wave-function-based methods, which naturally take into account the dispersion interactions, are too demanding for the oligomers investigated here. However, it is still possible to use a correction for DFT geometries and energies, at essentially no extra computational cost, to account for a large part of this contribution to the electronic energy. The dispersion energy between two weakly overlapping systems is thus calculated separately (in a post-SCF fashion) by resorting to a function which explicitly depends on the well-known R^{-6} decay of these interactions:

$$E_D = f_d(R)\frac{C_6}{R^6}, \quad (4)$$

where f_d (R) is a damping function of the interatomic distance (R) and C_6 is a dispersion coefficient [55–57]. We adopt this approach here, which is termed in general DFT–D, for the optimization of the π-stacked DBF systems. The method has been conveniently parameterized for the BLYP, B_λLYP ($\equiv$B3LYP), and B2-PLYP functionals [58].

We will thus systematically compare the structures calculated at the BLYP, B_λLYP, and B2-PLYP levels, with and without the dispersion correction, for molecules A, A′, and B; we choose two representative yet critical distances as a matter of example. First, we compare the distance between the quaternary carbon atoms of the fluorene rings (d_1), which experimentally (X-ray crystal structure) are known to be 2.61 Å (A), 2.70 Å (A′), and 2.73 Å (B). All the DFT methods employed lead to values very close to the experimental distances. For instance, the calculated distances for molecule A range from 2.68 (BLYP) to 2.62 Å (B_λLYP). The calculated distances oscillate for molecule A′ between 2.78 Å (BLYP) and 2.71 Å (B2-PLYP), and the same holds true for compound B. The dispersion correction, independently of the functional, always improves the data and brings them closer to experiments: 2.62–2.63 Å (A), 2.69–2.71 Å (A′) or 2.70–2.73 Å (B). Thus, the selection of exclusively this distance to assess the performance of a theoretical model chemistry, as done before [12], seems not to be enough to extract any conclusion about the reliability of the method to be used. However, since the fluorene moieties might adopt a face-to-face (syn configuration) or an edge-to-face (anti configuration) orientation, see Fig. 2 for the detailed investigated structures, we compare next for each molecule the distance between the carbon atoms being at the base of the pentagon of each fluorene ring (d_2). These distances are experimentally known to be: 5.79 ± 0.03 Å (A), 3.71 ± 0.01 Å (A′), and 3.75 ± 0.04 Å (B). Due to the interplay between the floppiness of the fluorene rings and the directionality of the non-covalent interactions, these distances appear to be much more sensitive to the method selected. In fact, this distance is calculated for molecule A to deviate by up to 0.3, 0.2, and 0.1 Å at the BLYP, B_λLYP, and B2-PLYP levels, respectively. Interestingly, the deviation reduces (in absolute value) to less than 0.1 Å if the dispersion correction is applied to any level. In the case of A′, the deviations are now 0.5, 0.4, and 0.1 Å at the BLYP, B_λLYP, and B2-PLYP level, respectively; which greatly reduce to an error of only 0.2 (0.1) Å after correcting the BLYP or B_λLYP (B2-PLYP) methods with the dispersion correction. Finally, the same degree of improvement found for A′ is also found for the trimer B. These results are collected in Table 3.

It should be noted that the theoretical results deviate the most for the molecules A′ and B; i.e., for those molecules for which the non-covalent interactions largely dominate

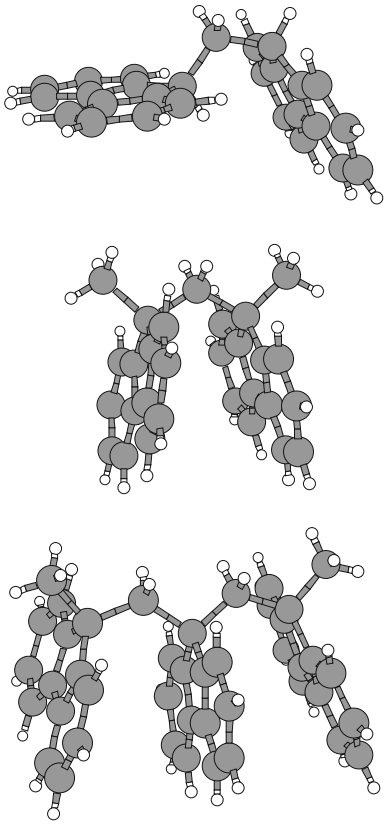

Fig. 2 Representation of the molecular geometries of compounds A, A′, and B (from *top* to *bottom*). The geometries shown come from crystal structures [9]. Figure created with XMakemol, see http://www.nongnu.org/xmakemol/

their shape. Furthermore, only the dispersion corrected methods are consistent with experimental findings. Thus, extreme care must be taken when using non-corrected, pure or hybrid GGAs, methods for DBF and closely related oligomers. As a compromise between accuracy and computational cost, we will thus use in the following the B_λLYP-D density functional, which is approximately an order of magnitude less costly than the corresponding B2-PLYP-D method, to robustly calculate the parameters relevant for charge transport rates and mobilities at the correct configuration.

3.3 Transport properties of π-stacked DBF oligomers

In the case of charge transport (CT) at room temperature, it is reasonable to consider that the rate of self-exchange electron-transfer reaction between two adjacent fluorene units (k^{CT}) can be described by the Marcus expression [59]:

$$k^{CT} = Ae^{-\lambda/4k_B\Theta}, \quad (5)$$

where the prefactor A depends on the strength of the electronic coupling, $A = f(t^2)$, in the case of a non-adiabatic process, Θ denotes the temperature, and k_B is the fundamental constant. The main two parameters defining the rate, and which thus deserve to be controlled or engineered by quantum-chemical methods, are λ, the total reorganization energy, and t, the electronic coupling, which is also called transfer integral. A large (moderate) value of the transfer integral (the reorganization energy) translates into a large hopping rate, which is closely related to the carrier mobilities. The validity of this approach is restricted by the condition $t < \lambda$ (*vide infra*).

The magnitude of λ reflects the changes occurring in the geometry of the interacting fluorene rings during the charge hopping (the internal part, λ_i) and the accommodation of the charge-induced changes by the surrounding medium (the external part, λ_s). The strategy to compute λ_i involves [60]: (i) the separate optimization of the geometry of the isolated neutral (E_{S_0}) and charged molecules (E_{D_0}); and (ii) the single-point calculations of the neutral molecule at the cation geometry ($E_{S_0//D_0}$) and of the charged molecule at the neutral geometry ($E_{D_0//S_0}$). Note that we primarily focus here on the internal part since λ_s is much less straightforward to calculate, it can be thus consider as a tunable parameter having a value of 0.2–0.4 eV, which is believed to be a highly realistic assumption [61]. Therefore, λ is then calculated as:

$$\lambda = \lambda_i + \lambda_s = \left(E_{D_0//S_0} - E_{D_0}\right) + \left(E_{S_0//D_0} - E_{S_0}\right) + \lambda_s \quad (6)$$

Accordingly with the results exposed in previous sections, since we need reliable geometries for the interacting pendants groups, the B_λLYP-D/6-31G* method was

Table 3 Calculated relevant distances: d_1 (distance between the quaternary carbon atoms of the fluorene rings, in Å) and d_2 (distance between the carbon atoms situated at the base of the pentagon of each fluorene ring, in Å)

Method	d_1			d_2		
	A	A′	B	A	A′	B
BLYP (–D)	2.68 (2.63)	2.78 (2.71)	2.80 (2.72)	6.07 (5.78)	4.23 (3.54)	4.13 (3.55)
B_λLYP (–D)	2.65 (2.62)	2.74 (2.69)	2.77 (2.70)	6.01 (5.76)	4.14 (3.54)	4.05 (3.55)
B2-PLYP (–D)	2.63 (2.63)	2.71 (2.71)	2.74 (2.73)	5.89 (5.89)	3.80 (3.80)	3.79 (3.79)
Exp.[a]	2.61	2.70	2.73	5.79	3.71	3.75

[a] Taken from [9]

consistently used for the calculation of λ_i. We obtain a value of 572 meV for the dimer A′, the prototype for the charge hopping occurring between adjacent fluorene units, which is admittedly larger than the values found for state-of-the-art molecules as oligo(acenes) and derivatives, TPD or titanyl phthalocyanines [21]. Interestingly, we have observed that the values obtained without the dispersion correction are underestimated by almost a factor of two, which might predict higher yet unrealistic values for the rate of hopping.

Figure 3 presents the shape of the orbitals involved in the hole transfer process, the Highest Occupied Molecular Orbital (HOMO) and the (H − 1)OMO, which are, however, asymmetrically distributed between the fluorene units for most of the oligomers unless for dimer A′. This molecule will be thus considered in the following as the model dimer for the rest of the oligomers. The transfer integral is calculated by a two-state model, combined with Koopmans' theorem, where the parameter t is estimated as half the splitting of the energies (ε) of the corresponding HOMO and (H − 1)OMO,

$$t = \frac{\varepsilon_{\mathrm{HOMO}} - \varepsilon_{(\mathrm{H}-1)\mathrm{OMO}}}{2}, \tag{7}$$

which is commonly known as the "energy splitting in dimer" (ESD) approximation [62]. We are aware that this way of calculating the coupling might overestimate the values in some cases [63], and especially when the fluorene units are not fully cofacial. Note also that the values of the calculated coupling might also depend on the theoretical method used to obtain the one-electron energies appearing in Eq. 7. The transfer integrals were obtained here from one-electron energies calculated at the Intermediate Neglect of Differential Overlap (INDO) level [64]. Even recognizing a slight dispersion of the results upon the method, the INDO-based values are typically of the same order of magnitude as those obtained with more sophisticated approaches [65, 66]. Furthermore, the choice of this method is motivated by the excellent compromise between accuracy and computational cost found in previous applications [67]; which is also validated here by comparing the available experimental gas-phase photoelectron spectra value (145 meV) of compound A′ [20] with the INDO estimate of 150 meV, obtained on the basis of the experimental geometry. Note that: (i) the B$_\lambda$LYP-D/6-31G* calculated value is slightly less accurate (90 meV); and (ii) we do not need to consider a more sophisticated three-state model [68] since the excess charge on the bridging group always remains lower than 0.02 |e|. The theoretical estimates of the effective electronic coupling are affected the most by the relative orientation of the fluorene rings. It is known that cofacial orientations of the rings in these systems would allow larger values but, in practise, the π-stacking is characterized by a rather flat potential energy surface with respect to the angle measuring the deviations from the cofacial orientation [20]. Additionally, the fluorene rings are progressively twisted, see Fig. 3, leading to a single-handed helical structure for the longest molecule. All these features might difficult the interpretation of the results and, shortly speaking, the estimate of 150 meV should be possibly considered as an upper limit.

Finally, the calculated values for the rate of intramolecular charge hopping, as obtained from Eqs. 5–7, range from 2.4×10^{11} s^{-1} ($\lambda_s = 0.2$ eV) to 3.1×10^{10} s^{-1} ($\lambda_s = 0.4$ eV), which are in the typical range expected for charge transport in the hopping regime [69]. Since the hole drift mobility of a π-stacked poly(dibenzofulvene) film was measured at 299 K to be as low as 2.7×10^{-4} cm^{2}V^{-1}s^{-1} [16], we compare next experimental and theoretical results,

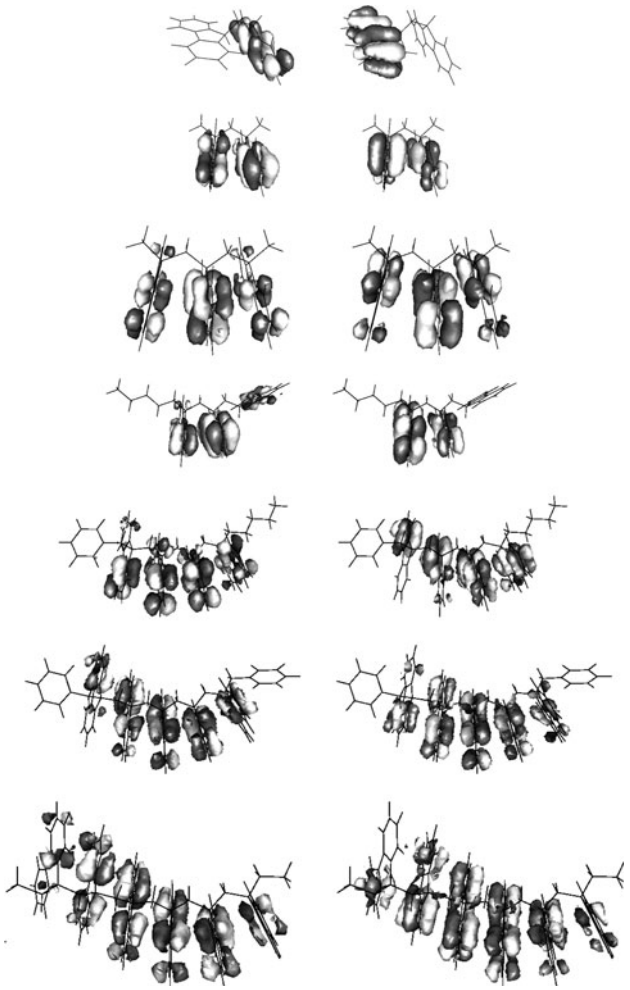

Fig. 3 Isocontour plots of the INDO/S//B$_\lambda$LYP-D/6-31G* calculated (H-1)OMO (*left*) and HOMO (*right*) molecular orbitals for the molecules A, A′, B, B′, C, D, and E (from *top* to *bottom*). The size and grey scale colour describe the amplitude and sign of the coefficients used to expand those π orbitals in terms of atomic orbitals. Figure created with gOpenMol, see http://www.csc.fi/english/pages/g0penMol/

assuming a purely diffusive motion of the charges, by feeding the results of the calculations into the following expression [70]:

$$\mu = \frac{ed^2}{k_B \Theta} k^{\mathrm{CT}}, \tag{8}$$

where d is the separation between the two moieties taking part in charge hopping (taken here as an average distance of 3.6 Å between all atoms belonging to the two adjacent fluorene rings in dimer A′) and k^{CT} is the formerly calculated rate. The hole mobilities estimated are found between 1.2×10^{-2} and 2.0×10^{-3} cm^2 V^{-1} s^{-1}; our theoretical calculations confirm than the mobilities experimentally found might well correspond to interchain charge transport, the slower process, whereas the intrachain process is characterized by (ideally) slightly larger mobilities. However, a competition between the two processes cannot be fully excluded from the present calculations; the control over the arrangements of the chains of poly(dibenzofulvene), or further derivatives, by fine-tuning of their alignment might induce higher mobilities and thus better efficiency for electronic devices.

We have finally investigated the effect of fusing benzene groups to the fluorene rings of the dimer A′, see Fig. 4 for the detailed structure of all the molecules considered (A′, A″, and A‴, from top to bottom), as an attempt to predict if such kind of molecular engineering would significantly affect the values of the reorganization energy: the calculated values for the molecules shown in Fig. 4 (from top to bottom) are 572, 360, and 315 meV, respectively. We can see how the energy dissipated after a sudden jump from the electronic state describing a hole in the donor molecule to that associated with a hole in the acceptor is largely affected in the right direction, as expected [71]. Note that for a reasonable INDO estimate of the transfer integral (t = 50–100 meV), see Table 4 for a summary of the results, considering that λ_s varies between 0.2 and 0.4 eV and taken again into account the difficulties arising from the floppiness of the cofacial rings, we calculate now transport rates between 3×10^{10} and 2×10^{12} s^{-1}. Thus, further molecular design by considering larger and more rigid pendant groups could also serve as a design guideline for novel functional materials belonging to this family of systems.

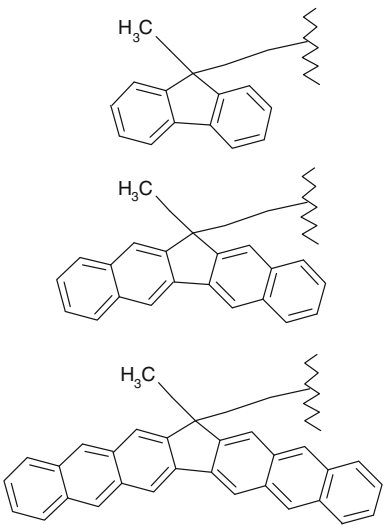

Fig. 4 Chemical structures of the engineered compounds. The hydrogen atoms have been omitted for clarity and only one-half of the molecule is shown

Table 4 Theoretical estimates of charge transport parameters: internal reorganization energy (λ, in meV) and transfer integral (t, in meV), see text for details

Molecule	λ	t
A′	572	150
A″	360	51
A‴	315	102

4 Conclusions

Oligo(dibenzofulvenes) have been studied as potential candidates to be used in devices for organic electronics. The face-to-face π-stacked fluorene rings promote a high degree of disorder leading to a helical-like shape for the longest oligomers. This feature prompted us to consider very accurate methods, specifically devised and systematically assessed for this kind of molecules, accounting for the all-pervasive non-covalent interactions which are expected to dominate the relative orientations of the fluorene rings. We have then calculated at the quantum-chemical level the reorganization energy and electronic coupling associated with intramolecular transport, which are found to strongly depend on the relative positions of the face-to-face π-stacked fluorene rings. Our calculations have yielded intramolecular or intrachain transport parameters (rate of charge transport and associated hole mobilities) which are slightly higher than the values experimentally found. The mobility results are consistent with a mechanism in which holes are expected to delocalize over π-stacked fluorene groups of the same chain, although the hopping between adjacent chains is possibly impeded by unfavourable intermolecular alignments; thus, hole transport along the conjugated polymer backbone might be significantly faster than hopping between neighbouring chains. This behaviour has been semi-quantitatively rationalized at a full quantum-chemical level, although for a quantitative comparison of intra- and intermolecular mobilities the detailed composition of the samples should be known at the nanoscale, which is missing at present. Therefore, the possible disorder of the chains in the film sample seems to act as a limiting step;

which, however, will not preclude the use of these π-stacked systems as molecular wires. It is also observed that condensing benzene groups at both ends of the fluorene rings seems to be also an efficient way to decrease the reorganization energies.

Acknowledgments The work in Alicante is supported by the "Ministerio de Educación y Ciencia" of Spain and the "European Regional Development Fund" through project CTQ2007-66461/BQU. J.C.S.G. thanks the "Ministerio de Educación y Ciencia" of Spain for a research contract under the "Ramón y Cajal" program and to the "Generalitat Valenciana" for further economic support. Useful discussions with J. Cornil and Y. Olivier (University of Mons-Hainaut, Belgium) and A. J. Pérez-Jiménez (University of Alicante, Spain) are also acknowledged.

References

1. Murphy AR, Fréchet JMJ (2007) Chem Rev 107:1066
2. Anthony JE (2008) Angew Chem Int Ed 47:452
3. Barbara PF, Meyer TJ, Ratner MA (1996) J Phys Chem 100:13148
4. Mas-Torrent M, Hadley P, Bromley ST, Ribas X, Tarrés J, Mas M, Molins E, Veciana J, Rovira C (2004) J Am Chem Soc 126:8546
5. Reese C, Bao Z (2006) J Mater Chem 16:329
6. da Silva Filho DA, Kim E-G, Bredás JL (2005) Adv Mater 17:1072
7. Li L, Tang Q, Li H, Yang X, Hu W, Song Y, Shuai Z, Xu W, Liu Y, Zhu D (2007) Adv Mater 19:2613
8. Norton JE, Brédas JL (2008) J Chem Phys 128:034701
9. Rathore R, Abdelwahed SH, Guzei IA (2003) J Am Chem Soc 125:8712
10. Nakano T, Yade T (2003) J Am Chem Soc 125:15474
11. Nakano T, Yade T, Fukuda Y, Yamaguchi T, Okomura S (2005) Macromolecules 38:8140
12. Kim WS, Kim J, Park KK, Mukamel S, Rhee SK, Choi YK, Lee JY (2005) J Phys Chem A 109:2686
13. Nakano T, Nakagawa O, Tsuji M, Tanikawa M, Yade T, Okamoto Y (2004) Chem Commun 144
14. Nakano T, Tanikawa M, Nakagawa O, Yade T, Sakamoto T (2009) J Polym Sci Part A: Polym Chem 47:239
15. Xie L-H, Deng X-Y, Chen L, Chen S-F, Liu R-R, Hou X-Y, Wong K-Y, Ling Q-D, Huang W (2009) J Polym Sci Part A: Polym Chem 47:5221
16. Nakano T, Yade T, Yokoyama M, Nagayam N (2004) Chem Lett 33:296
17. van Vooren A, Kim J-S, Cornil J (2008) Chem Phys Chem 9:989
18. Rathore R, Abdelwahed SH, Kiesewetter MK, Reiter RC, Stevenson CD (2006) J Phys Chem B 110:1536
19. Yan S, Lee SJ, Kang S, Lee JY (2007) Supramol Chem 19:229
20. Coropceanu V, Nakano T, Gruhn NE, Kwon O, Yade T, Katsukawa K-I, Brédas J-L (2006) J Phys Chem B 110:9482
21. Coropceanu V, Cornil J, da Silva Filho DA, Olivier Y, Silbey R, Bredás JL (2007) Chem Rev 107:926
22. Becke AD (1988) Phys Rev A 38:3098
23. Lee C, Yang W, Parr RG (1988) Phys Rev B 37:785
24. Grimme S (2006) J Chem Phys 124:034108
25. Kohn W, Sham LJ (1965) Phys Rev A 140:1133
26. Perdew JP, Schmidt K (2001) In: Van Doren V et al. (eds) Density functional theory and its application to materials. American Institute of Physics, Melville
27. Kummel S, Kronik L (2008) Rev Mod Phys 3:80
28. Schwabe T, Grimme S (2008) Acc Chem Res 41:569
29. Sancho-García JC, Pérez-Jiménez AJ (2009) J Chem Phys 131:084108
30. Zhang Y, Xu X, Goddard WA III (2009) Proc Natl Acad Sci USA 106:4963
31. Sancho-García JC (2007) Chem Phys 331:321
32. Becke AD (1993) J Chem Phys 98:5648
33. Černý J, Hobza P (2007) Phys Chem Chem Phys 9:5291
34. Neese F (2006) ORCA—an ab-initio, density functional and semi-empirical program package, version 2.6.35. University of Bonn
35. Neese F, Schwabe T, Grimme S (2007) J Chem Phys 126:124115
36. Neese F (2003) J Comp Chem 24:1740
37. Eichkorn K, Treutler O, Öhm H, M. Häser, Ahlrichs R (1995) Chem Phys Lett 240:283
38. Huang J, Kertesz M (2004) Chem Phys Lett 390:110
39. Chen H-Y, Chao I (2005) Chem Phys Lett 401:539
40. Sancho-García JC, Horowitz G, Brédas JL, Cornil J (2003) J Chem Phys 119:12563
41. Valero R, Costa R, de Moreira PR I, Truhlar DG, Illas F (2008) J Chem Phys 128:114103
42. Deleuze MS, Claes L, Kryachko ES, François J-P (2003) J Chem Phys 119:3106
43. Gierschner J, Cornil J (2007) Adv Mater 19:173
44. Bredás JL, Beljonne D, Coropceanu V, Cornil J (2004) Chem Rev 104:4971
45. van Leeuwen R, Baerends EJ (1994) Phys Rev A 49:2421
46. Grüning M, Gritsenko OV, van Gisbergen SJA, Baerends EJ (2001) J Chem Phys 114:652
47. Grimme S, Neese F (2007) J Chem Phys 127:154116
48. Dierksen M, Grimme S (2004) J Phys Chem A 108:10225
49. Sancho-García JC (2007) Chem Phys Lett 439:236
50. Sancho-García JC, Pérez-Jiménez AJ (2008) J Chem Phys 129:024103
51. Cozzi F, Annunziata R, Benaglia M, Baldridge KK, Aguirre G, Estrada J, Sritana-Anant Y, Siegel JS (2008) Phys Chem Chem Phys 10:2686
52. Grimme S, Antony J, Schwabe T, Mück-Lichtenfeld C (2007) Org Biomol Chem 5:741
53. Fink RF, Seibt J, Engel V, Renz M, Kaupp M, Lochbrunner S, Zhao HM, Pfister J, Würthner F, Engels B (2008) J Am Chem Soc 130:12858
54. Zhao H-M, Pfister J, Settels V, Renz M, Kaupp M, Dehm VC, Würthner F, Fink RF, Engels B (2009) J Am Chem Soc 131:15660
55. Wu Q, Yang W (2002) J Chem Phys 116:515
56. Grimme S (2006) J Comput Chem 27:1787
57. Jurečka P, Černý J, Hobza P, Salahub DR (2007) J Comput Chem 28:555
58. Schwabe T, Grimme S (2007) Phys Chem Chem Phys 9:3397
59. Marcus RA (1965) J Chem Phys 24:966
60. Berlin Y, Hutchinson GR, Rempala P, Ratner MA, Michl J (2003) J Phys Chem A 107:3970
61. Lemaur V, Steel M, Beljonne D, Brédas JL, Cornil J (2005) J Am Chem Soc 127:6077
62. Newton MD (1991) Chem Rev 91:767
63. Valeev EF, Coropceanu V, da Silva Filho DA, Salman S, Brédas JL (2006) J Am Chem Soc 128:9882
64. Ridley J, Zerner MC (1973) Theor Chim Acta 32:111
65. Rodríguez-Monge L, Larsson S (1996) J Phys Chem 100:6298
66. Blancafort L, Voityuk AA (2006) J Phys Chem A 110:6246
67. van Vooren A, Lemaur V, Ye A, Beljonne D, Cornil J (2007) Chem Phys Chem 8:1240
68. Voityuk AA (2008) Chem Phys Lett 451:153
69. Olivier Y, Lemaur V, Brédas JL, Cornil J (2006) J Phys Chem A 110:6356
70. Grozema FC, Siebbeles LDA (2008) Int Rev Phys Chem 27:87
71. Devos A, Lannoo M (1998) Phys Rev B 58:8236